Progress In Electromagnetics Research Letters, Vol. 126, 9–15, 2025

PIER Letters

(Received 4 March 2025, Accepted 16 April 2025, Scheduled 26 April 2025)

3D Printed Waveguide Antenna at X-Band Frequency Band Using MSLA Printing Technology

Huda A. Majid[1,*], Fahmiruddin Esa[2], Herdawatie A. Kadir[3], Azka Rehman[2], Hilman Harun[4], Muzammil Jusoh[5], Najib Al-Fadhali[6], Dian W. Astuti[7], and Noor A. Shairi[8]

[1]*Faculty of Engineering Technology, Universiti Tun Hussein Onn Malaysia Pagoh Higher Education Hub, Pagoh, Johor 84600, Malaysia*
[2]*Faculty of Science and Technology, Universiti Tun Hussein Onn Malaysia Pagoh Higher Education Hub, Pagoh, Johor 84600, Malaysia*
[3]*Faculty of Electrical and Electronic Engineering, Universiti Tun Hussein Onn Malaysia Parit Raja, Johor 86400, Malaysia*
[4]*Mindmatics Sdn Bhd, Taman Kajang Sentral, Kajang, Selangor 43000, Malaysia*
[5]*Faculty of Electronic Engineering Technology, Universiti Malaysia Perlis, Arau, Perlis 02600, Malaysia*
[6]*Electrical Engineering Technology, Alfred State College of Technology State University of New York, NY 14802, United States*
[7]*Department of Electrical Engineering, Faculty of Engineering, Universitas Mercu Buana, Indonesia*
[8]*Centre for Telecommunication Research and Innovation (CeTRI) Fakulti Teknologi dan Kejuruteraan Elektronik dan Komputer (FTKEK) Universiti Teknikal Malaysia Melaka (UTeM), Melaka, Malaysia*

ABSTRACT: Rapid advancements in 3D printing technology have revolutionized antenna fabrication, allowing for the creation of intricate, lightweight, and high-performance structures with exceptional precision. This paper presents the design, fabrication, and experimental evaluation of a 3D-printed waveguide antenna operating in the X-band frequency range (8–11 GHz). The antenna was manufactured using Masked Stereolithography Apparatus (MSLA) technology with Magma X 12 K Dura ABS resin, which was selected for its excellent mechanical strength and dielectric properties. A 0.2 mm thick silver conductive coating was applied to enhance the electrical conductivity and minimize the surface resistance. The proposed antenna is based on a WR-90 rectangular waveguide configuration with an optimized aperture, which ensures minimal reflection loss and high radiation efficiency. Experimental results indicate an impedance bandwidth of 1.34 GHz, spanning from 8.56 GHz to 9.9 GHz, with an optimal resonant frequency at 9.45 GHz. The measured and simulated S_{11} parameters exhibited strong agreement, validating effective impedance matching and minimal energy dissipation. Furthermore, radiation pattern analysis revealed a directional gain of 6.85 dBi and an overall radiation efficiency of 98.35%. The measured 3 dB beamwidths were 60.5° in the E-plane and 105.8° in the H-plane, confirming the suitability of the antenna for applications in satellite communication, radar, and wireless sensing. The results demonstrate the viability of MSLA-based additive manufacturing for high-frequency waveguide antennas, offering a cost-effective, lightweight, and high-performance alternative to the traditional fabrication techniques. This study highlights the potential of 3D printing as an innovative approach for the development of next-generation microwave and millimeter-wave communication systems.

1. INTRODUCTION

The rapid advancement in 3D printing technology and manufacturing has revolutionized antenna design, enabling the fabrication of complex and high-performance structures with greater precision and efficiency [1]. This technology has led to several advantages in aerospace, defense, satellite communication, and radar systems due to their lightweight, fast prototyping and cost-effectiveness [2, 3]. Traditional antenna manufacturing methods often involve complex machining and assembly [4–6], whereas 3D printing allows for seamless integration of intricate geometries, dielectric materials, and conformal designs. One of the key advantages of 3D printing in antenna design is its ability to create intricate and lightweight structures. This is particularly important in applications where weight and size are critical, such as the aerospace and automotive sectors. 3D printing allows for the creation of complex shapes and geometries that can optimize antenna performance, leading to improved radiation patterns, gain, and efficiency [7].

Over the past few years, 3D printing has been used for the design and fabrication of antennas. Hamdalla et al. designed a low-profile wideband metasurface antenna for high-power applications [8]. An N-type-to-waveguide transition was used to excite the metasurfaces, and a 4×4 array of unit cells was integrated into a 3D-printed waveguide. The internal faces of the waveguide were covered with copper tape to minimize the weight. Experimental testing demonstrated functionality from 2.1 GHz to 3.6 GHz (52.6% bandwidth), with a peak gain of 8.5 dBi. The high-power handling capability of the antenna suggests its suitability for radar applications and Unmanned Aerial Vehicle (UAV) communication. Ghosh and Harack-

* Corresponding author: Huda Abdul Majid (mhuda@uthm.edu.my).

iewicz fabricated a low-profile strip-based helical antenna using 3D printing technology [9]. The fabricated antenna was constructed with two independent conductive elements, achieving a wide impedance bandwidth of 99%, maximum gain of 9.40 dBi, and beamwidth of approximately 60°. Researchers have leveraged the flexibility of 3D printing to create a non-planar helical structure, which is typically challenging to fabricate using traditional methods because of the precise alignment and spacing required between conductive elements, especially in the strip form. These antennas were printed using Polylactic Acid (PLA) material. Yamoun & Aknin introduced a 3D-printed ring dielectric resonator antenna constructed using Acrylonitrile Butadiene Styrene (ABS) filament [10]. The antenna exhibits two resonant frequencies at 23.5 GHz and 26.4 GHz, with respective gains of 9.5 dB and 10.5 dB, achieving a wide bandwidth of 42.4%. The authors leveraged 3D printing technology to fabricate the ring Dielectric Resonator Antenna (DRA), taking advantage of the ease of fabrication and ability to create complex antenna shapes. The choice of printing material or filament is crucial in 3D-printed antenna design because it directly affects the antenna's material characteristics, such as the dielectric constant, loss tangent, and structural integrity. For instance, materials such as Acrylonitrile Butadiene Styrene are favored for their durability, temperature resistance, and low tangent loss, whereas Polylactic Acid offers ease of printing, but may exhibit higher losses [9, 10]. The material properties influence the antenna bandwidth, gain, and efficiency, making material selection a critical design consideration.

Furthermore, the most commonly used and cost-effective processes are Fused Deposition Modeling (FDM) and stereolithography apparatus (SLA) [11–13]. SLA is generally superior to FDM in terms of precision, surface quality, and material properties, making it the preferred choice for applications that require high accuracy and fine details [14]. SLA uses an ultraviolet (UV) light source, which is then selectively masked with an LCD screen to cure the liquid resin layer by layer, achieving significantly higher resolution and smoother surfaces than FDM, which extrudes thermoplastic filaments layer by layer, often resulting in visible layer lines and lower detail accuracy [15]. Although FDM is more affordable and easier to use, its lower precision and surface finish make it unsuitable for antenna design applications. SLA, which uses UV light to cure liquid resin layer-by-layer, offers superior resolution and smoother surfaces, making it the preferred choice for intricate antenna designs [16, 17]. An advanced variation of SLA, Masked Stereolithography Apparatus (MSLA), utilizes an LCD screen to selectively mask UV light and cure entire layers simultaneously [18]. This approach offers faster and more precise fabrication than traditional SLA and Digital Light Processing (DLP) techniques [19]. The MSLA can produce smooth, geometrically intricate structures, making it particularly well suited for X-band waveguide antennas by minimizing the surface roughness and optimizing the electromagnetic performance [1]. Moreover, their improved fabrication efficiency and material versatility further reinforce their suitability for high-frequency applications.

This study focuses on the design, fabrication, and performance evaluation of a 3D-printed X-band waveguide antenna (8–11 GHz) utilizing MSLA technology with Magma X 12 K Dura ABS resin, which was selected for its superior mechanical strength and dielectric stability. A 0.2 mm silver coating was applied to enhance the conductivity and minimize the surface resistance. The design of the WR-90 waveguide was optimized for minimal loss and high radiation efficiency. Experimental validation, supported by simulations, demonstrated strong impedance matching, high gain, and excellent radiation efficiency, thereby confirming the feasibility of MSLA-based additive manufacturing for high-frequency applications. The results highlight the potential of 3D printing as a scalable, lightweight, and cost-effective alternative to conventional antenna fabrication methods, with promising applications in satellite communication, radar, UAV systems, and wireless sensing.

2. ANTENNA DESIGN AND FABRICATION

A schematic of the proposed 3D-printed waveguide antenna, suitable for operation within the X-band frequency range (8–11 GHz), is shown in Figure 1. The height of the waveguide antenna was 14.10 mm, width of the base was 26.80 mm, and length of the structure was 60.03 mm. Internally, within the aperture of the guide, there is a vertical aperture of 10.10 mm and a horizontal slot of 22.80 mm, which allows proper propagation of electromagnetic waves and impedance matching in the X-band [20].

The structural configurations and design features of the fabricated 3D-printed waveguide antennas with different orientations are shown in Figure 2. The classification, measurement, and feeding techniques used in the design were combined as shown in Figures 2(a), (b), and (c). They depict the waveguide feed port along with the output matching section and aperture, which focuses in a specific direction for electromagnetic energy radiation. The taper at the aperture, as illustrated in Figure 2(c), is specifically designed to provide impedance matching between the waveguide and free space, thereby minimizing reflection and maximizing the efficiency of power transfer from the antenna. This gradual transition in geometry helps to smooth the impedance variation seen by the propagating wave, ensuring a broader operational bandwidth. The exact dimensions and proportions of the antenna can be preserved during the 3D printing process, making this technology useful for the fabrication of lightweight and high-functioning antennas [21, 22].

The precise dimensions of the coaxial-to-waveguide transition that optimally couples the electromagnetic (EM) signal on the coaxial feed to the waveguide structure are shown in Figure 3. The stepped ridge transformer was designed to facilitate low insertion loss and impedance matching with a 50 Ω coaxial connector [23]. The number of ridge steps is three, with each element having an optimized length of one quarter of the guide wavelength. The inner conductor of the coaxial line extends axially into the waveguide and connects to the final ridge. The height of each ridge is optimized to get the best matching impedance. The stepped ridge transformer converts the transverse electromagnetic (TEM) mode of the coaxial connector to the TE_{10} dominant mode. Furthermore, the WR-90 waveguide

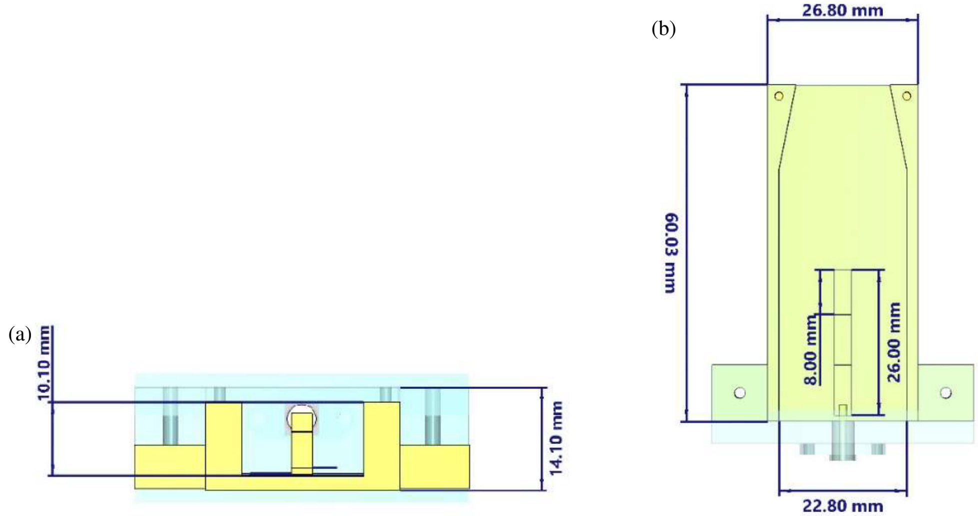

FIGURE 1. Dimension (a) side view and (b) top view of the 3D printed waveguide antenna.

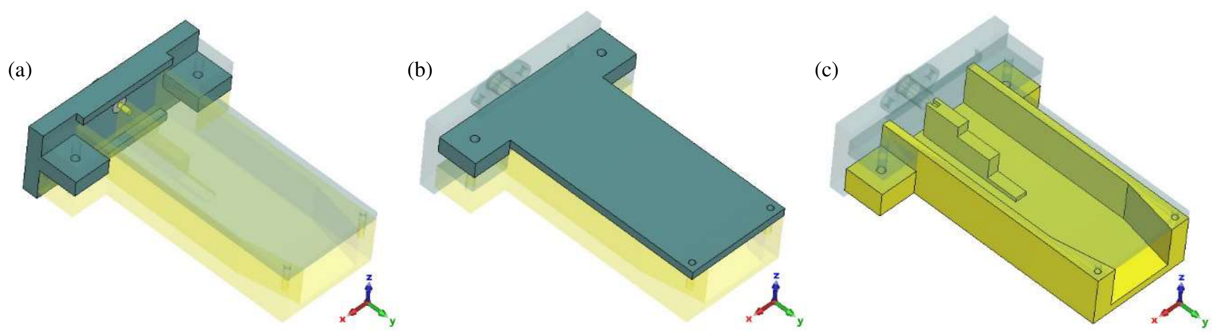

FIGURE 2. Perspective view of the 3D printed waveguide antenna (a) end-cap, (b) top, (c) base of the waveguide.

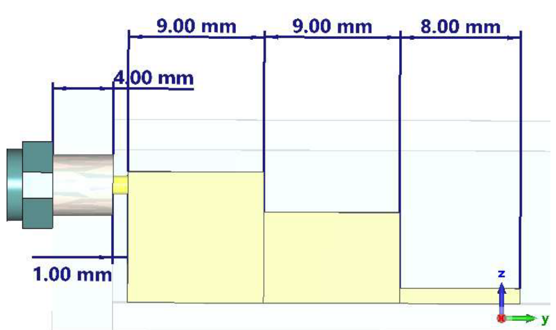

FIGURE 3. Dimension of the stepped ridge transformer (coaxial to waveguide transition).

with standard dimension of 22.8 mm $\times$ 10.1 mm operates in the X-band 8 to 11 GHz frequency range.

A 3D-printed waveguide antenna, developed according to the design parameters, is shown in Figure 4. The antenna is designed in the form of a rectangular waveguide with standard measurements of a WR-90 waveguide with an overall length of 50 mm, width of 22.8 mm, and height of 10.1 mm [24]. In addition, the aperture dimensions were optimized to yield high radiation efficiency and low reflection losses. The antenna components were 3D printed to achieve complex and specific details while maintaining a low weight [25]. The used 3D printer was Elegoo Saturn 2. Elegoo Saturn 2 is an MSLA resin 3D printer featuring a 7680×4320 resolution, delivering 28.5-micron XY precision for highly detailed prints. MSLA photocuring is a 3D printing technique that uses UV light to harden a photopolymer resin into a 3D shape. MSLA technology enables faster and more precise fabrication than the traditional SLA and DLP methods. For this purpose, the Magma X 12 K Dura ABS resin was selected because of its outstanding mechanical strength, thermal stability, and favourable dielectric properties, making it highly suitable for high-frequency antenna applications. Its low dielectric loss and high durability are essential for preserving the signal integrity and minimizing propagation losses. Additionally, its fine resolution ensures a smooth surface finish, reduces scattering losses, and enhances overall antenna performance. The combination of MSLA printing technology and high-performance resin allows the fabrication of intricate, high-precision antenna structures while maintaining cost-effectiveness, making it a promising approach for advanced waveguide antenna applications.

To enhance the conductivity and decrease the surface resistance, approximately 0.2 mm thick silver conductive surface coatings were coated on the surface of the 3D printed structure. These coatings significantly reduced propagation losses.

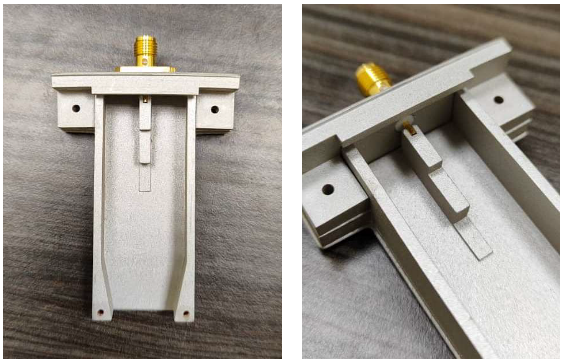

FIGURE 4. Fabricated proposed antenna.

TABLE 1. Error margin of the dimension between fabricated and simulated antenna.

Parameters	Dimension Error Margin %
Aperture height	3.8
Aperture width	1.1
Wall thickness	5.0
Stepped ridge height	1.5
Stepped ridge thickness	6.7
Stepped ridge length	0.4

The antenna is equipped with a coaxial-to-waveguide transition, which allows impedance matching between the waveguide and 50 Ω coaxial feed. The fabricated antenna yielded superior radiation characteristics with specific and directional patterns, making it suitable for wireless sensing, satellite communication, and radar [26]. Additive manufacturing (3D printing) with a conductive coating was validated, along with design feasibility, which provides a budget-friendly, lightweight, and high-functioning solution for X-band frequency applications. Furthermore, the dimensions of the fabricated antenna were measured using a digital vernier calliper. The dimensional discrepancies between the fabricated and simulated antennas are presented in Table 1. The listed dimensions represent the most critical parameters influencing the antenna's resonant frequency and impedance matching. The higher margin of error observed is primarily attributed to the thickness of the silver conductive surface coating applied during fabrication.

3. SIMULATION AND RESULT

The simulated and measured reflection coefficients of the proposed antenna in the frequency range are shown in Figure 5. The assessment of the calculated and obtained S_{11} results from the measurements within the X-band frequency range shows that the results are in excellent agreement with one another and that the deviation is nominal. The slight shifts between the simulated and actual results were due to environmental conditions during testing, which corroborates the accuracy and quality of the fabrication process [27]. The proposed antennas were found

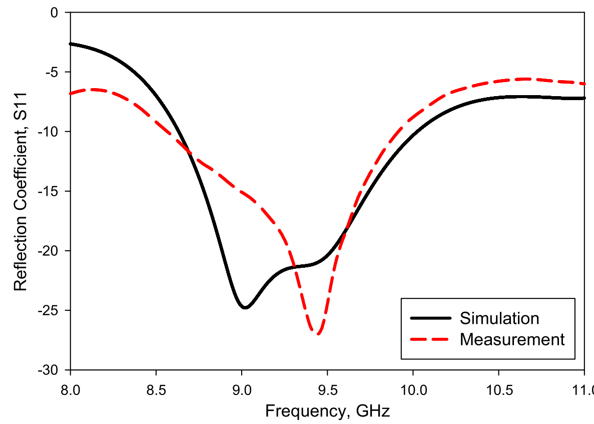

FIGURE 5. Comparison between simulated and measured reflection coefficients, S_{11}.

to exhibit good return loss (S_{11} is less than -10 dB), which is expected in the wide band. The measured impedance bandwidth is 1.34 GHz, while the lower bound is at a frequency of 8.56 GHz and the upper bound at a frequency of 9.9 GHz. The impedance bandwidth error margin between the simulated and measured results is only 1.47%. A resonant frequency of 9.45 GHz was found to be optimal for impedance matching, such that energy transfer was effective; outflow was minimal; and the overall performance was optimal.

The 3D radiation pattern in Figure 6 verifies that the antenna functions as a directional antenna with a gain of 6.85 dBi. The significance of these results is that they prove the efficiency of the proposed methodology and its feasibility for the design of high-performance antennas for X-band applications. In this case, the antenna demonstrated a simulated total radiation efficiency of -0.072 dB which was approximately 98.35%.

Figures 7 and 8 show polar plots of simulated and measured 2D radiation patterns captured in the E and H planes, respectively, for the waveguide antenna in the 9.45 GHz band. The E-plane is the yz-plane (refer to axis in Figure 6), while the H-plane, shows the radiation pattern in the xy-plane. The measured radiation pattern is shown by a black solid line, whereas

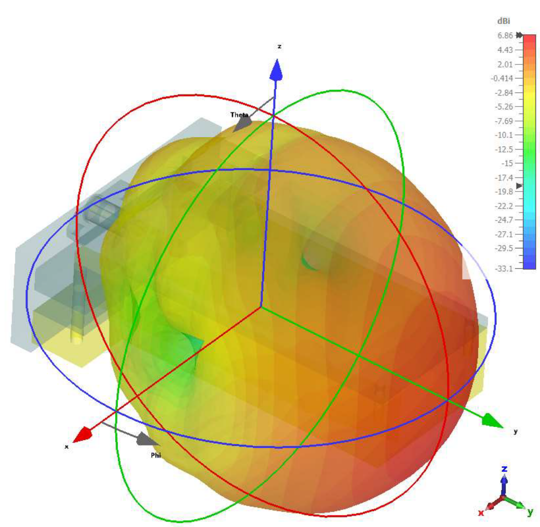

FIGURE 6. 3D radiation pattern of the proposed antenna at 9.45 GHz.

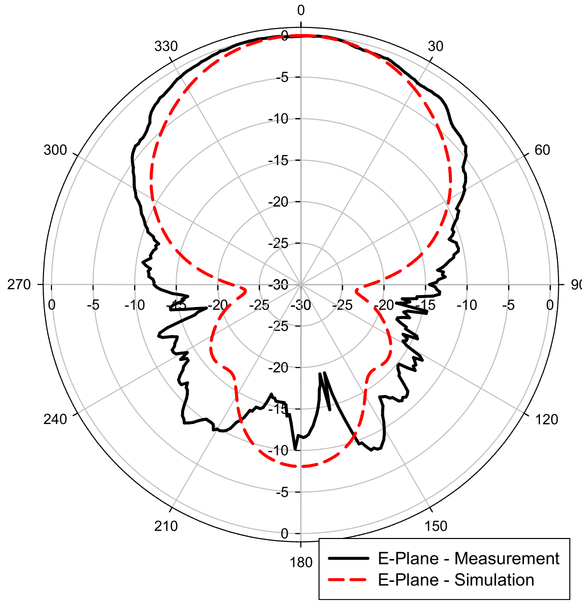

FIGURE 7. Simulated and measured radiation patterns in E-plane at 9.45 GHz.

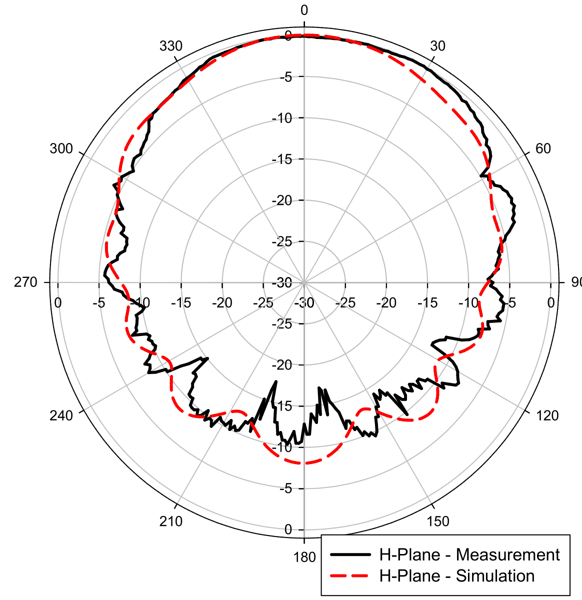

FIGURE 8. Simulated and measured radiation patterns in H-plane at 9.45 GHz.

TABLE 2. Comparison with other related works.

References	Size (mm)	Bandwidth	Gain	Radiation Efficiency
SLM 3D-Printed Horn Antenna for Satellite Communications at X-band [29]	$247.79 \times 100 \times 100$	7.5–11.5 GHz	18 dB	-
Use of 3D Printing for Horn Antenna Manufacturing [30]	$100 \times 20 \times 40$	8 to 11.3 GHz	11.5 dBi	-
3D print X-band horn antenna for ground-based SAR application [31]	$60 \times 40 \times 40$	8 to 10.5 GHz	15.3 dBi	$> 90\%$
Proposed Antenna	$60 \times 10 \times 30$	8.56 to 9.9 GHz	6.85 dBi	98.35%

the simulated pattern is represented by a red dashed line. The patterns exhibited strong agreement, thereby demonstrating the accuracy of the design and simulation models. Meanwhile, the measured data exhibited some distortion and fluctuation owing to the environmental reflection [28]. The E- and H-planes ensure that the antenna radiation pattern is properly captured. In the E-plane, the antenna 3 dB half-power beamwidth was 60.5°, whereas in the H-plane, the 3 dB half-power beamwidth was 105.8°. The projected data show that the proposed 3D-printed waveguide antenna achieves good directional radiation, and the numerically simulated results agree with physical measurements. Table 2 shows the comparison with other related works. The proposed antenna offers notable advantages in terms of compact size and high radiation efficiency. Measuring just $60 \times 10 \times 30$ mm, it is significantly smaller than other compared designs, making it ideal for compact and portable applications. It operates within the X-band (8.56–9.9 GHz) and achieves a high radiation efficiency of 98.35%, the highest among all listed antennas. Although its gain (6.85 dBi) is lower, this is a reasonable trade-off considering its small form factor and exceptional efficiency.

4. CONCLUSION

This study successfully demonstrates the design, fabrication, and performance evaluation of a 3D-printed waveguide antenna tailored for X-band (8–11 GHz) applications. The fabricated antenna exhibits excellent mechanical strength, dielectric stability, and structural precision when employing MSLA technology with Magma X 12 K Dura ABS resin. The application of a 0.2 mm silver conductive coating significantly enhanced the electrical conductivity, minimized propagation losses, and ensured optimal electromagnetic performance. The experimental results validate the effectiveness of the antenna with a measured impedance bandwidth of 1.34 GHz (8.56 GHz–9.9 GHz) and an optimal resonant frequency of 9.45 GHz. The close correlation between the simulated and measured S_{11} parameters confirms effective impedance matching with minimal insertion loss. Additionally, the antenna achieves a directional gain of 6.85 dBi and an impressive radiation efficiency of 98.35%, reinforcing its suitability for high-frequency applications. The well-formed radiation pattern, characterized by 3 dB beamwidths of 60.5° in the E-plane and 105.8° in the H-plane, ensured efficient energy transmission. These findings highlight the potential of MSLA-based additive manufacturing for high-performance, advanced microwave applications. Compared to conventional fabrication techniques, 3D printing offers remarkable advantages, including design flexibility, rapid prototyping, material efficiency, and reduced weight, without compromising structural integrity. These results pave the way for the widespread adoption of 3D-printed antennas in satellite communication, radars, UAV systems, and wireless sensing applications. For satellite communication and radar applications, specific design considerations such as structural ruggedness, integration with phased array systems, and low-profile or conformal geometries should be addressed. Although the MSLA technology with Dura ABS resin showed promising mechanical and dielectric properties, the study was confined to this specific material and printing method. Exploring alternative 3D printing materials, including those with higher temperature stability, may further improve antenna performance and usage for industry and outdoor applications. Additionally, while the application of a silver conductive coating enhanced conductivity and reduced propagation losses, other types of conductive coatings or metallization techniques could be investigated for better efficiency, ease of application, and long-term durability. In summary, further work involving material exploration and alternative surface treatments is recommended to advance the development of 3D-printed antennas for high-frequency and mission-critical applications such as in satellite communication and radar system.

ACKNOWLEDGEMENT

This research was supported by Universiti Tun Hussein Onn Malaysia (UTHM) through MDR (vot Q694).

REFERENCES

[1] Richhariya, G., R. K. Shukla, M. Sawale, N. Vishwakarma, and N. Singh, "Recent trends in 3D printing antennas," in *Array and Wearable Antennas*, 218–233, CRC Press, 2024.

[2] Siengchin, S., "A review on lightweight materials for defence applications: Present and future developments," *Defence Technology*, Vol. 24, 1–17, 2023.

[3] Masrafee, M. M. R., A. B. Rashid, and M. E. Hoque, "Innovations in 3D printing-assisted biopolymer composites for aerospace applications," in *Sustainable 3D Printing for Innovative Biopolymer Production and Applications*, 117–147, Chapter 6, Wiley, 2025.

[4] Gupta, A., V. Kumar, S. Bansal, M. H. Alsharif, A. Jahid, and H.-S. Cho, "A miniaturized tri-band implantable antenna for ISM/WMTS/lower UWB/Wi-Fi frequencies," *Sensors*, Vol. 23, No. 15, 6989, 2023.

[5] Gupta, A., M. Aljaidi, S. Bansal, R. E. A. Mamlook, V. Kumar, A. Aljohani, S. Aljohani, and M. K. Singla, "Design analysis and performance enhancement of a 2-element MIMO skin-implantable antenna for IoT-based health monitoring devices," *PLoS One*, Vol. 19, No. 12, e0311753, Dec. 2024.

[6] Chaparala, R., S. Imamvali, S. Tupakula, K. Prakash, S. Bansal, M. M. Ismail, and A. J. A. Al-Gburi, "Spoof surface plasmon polaritons-based feeder for a dielectric rod antenna at microwave frequencies," *Progress In Electromagnetics Research M*, Vol. 129, 23–32, 2024.

[7] Mohanavel, V., K. S. A. Ali, K. Ranganathan, J. A. Jeffrey, M. M. Ravikumar, and S. Rajkumar, "The roles and applications of additive manufacturing in the aerospace and automobile sector," *Materials Today: Proceedings*, Vol. 47, 405–409, 2021.

[8] Hamdalla, M. Z. M., M. Zawad, M. Kunkle, S. Baidya, R. C. Allen, P. J. Bland, T. D. Fields, and A. M. Hassan, "Design of a 3D printed wide band metasurface antenna for high power applications," *Progress In Electromagnetics Research M*, Vol. 128, 115–125, 2024.

[9] Ghosh, P. and F. Harackiewicz, "3D printed low profile strip-based helical antenna," *Progress In Electromagnetics Research C*, Vol. 127, 195–205, 2022.

[10] Yamoun, J. B. and N. Aknin, "3D printed wideband ring dielectric resonator antenna," *Progress In Electromagnetics Research Letters*, Vol. 114, 97–102, 2023.

[11] Kronberger, R., S. Grünwald, V. Wienstroer, and V. Tsatsos, "New low-cost FDM technology for printing antennas," in *2020 International Symposium on Antennas and Propagation (ISAP)*, 571–572, Osaka, Japan, 2021.

[12] Li, S., B. S. Izquierdo, S. Gao, and Z. Chen, "Analysis of 3D printed dielectric resonator antenna arrays for millimeter-wave 5G applications," *Applied Sciences*, Vol. 14, No. 21, 9886, 2024.

[13] Shou, Z., Z. Wu, H. Wang, H. Zhou, and M. Hou, "Design of the 3D-printed rectangular dielectric resonator antenna for WLAN applications," in *2024 18th European Conference on Antennas and Propagation (EuCAP)*, 1–4, Glasgow, United Kingdom, 2024.

[14] Carvalho, S. S., J. R. V. Reis, A. Mateus, and R. F. S. Caldeirinha, "Exploring design approaches for 3D printed antennas," *IEEE Access*, Vol. 12, 10 718–10 735, 2024.

[15] Mhmood, T. R. and N. K. Al-Karkhi, "A review of the stereo lithography 3D printing process and the effect of parameters on quality," *Al-Khwarizmi Engineering Journal*, Vol. 19, No. 2, 82–94, 2023.

[16] Tamayo-Domínguez, A., J. M. F. González, and M. Sierra-Castañer, "Stereolithography and direct metal laser sintering applied to mm-Wave antennas," in *2020 International Symposium on Antennas and Propagation (ISAP)*, 273–274, Osaka, Japan, 2021.

[17] Basile, V., M. Grande, V. Marrocco, D. Laneve, S. Petrignani, F. Prudenzano, and I. Fassi, "Design and manufacturing of super-shaped dielectric resonator antennas for 5G applications using stereolithography," *IEEE Access*, Vol. 8, 82 929–82 937, 2020.

[18] Popescu, V.-S. and I.-M. Popescu, "Impact of UV post processing on simple 3D printed parts using masked stereolithography," *International Journal of Mechatronics and Applied Mechanics*, No. 18, 86–92, 2024.

[19] Divjak, A., M. Matijević, and K. Hajdek, "Review of photopolymer materials in masked stereolithographic additive manufacturing," in *11th International Symposium on Graphic Engineering and Design (GRID 2022)*, 431–438, Novi Sad, Serbia, 2022.

[20] Alkaraki, S., Y. Gao, S. Stremsdoerfer, E. Gayets, and C. G. Parini, "3D printed corrugated plate antennas with high aperture efficiency and high gain at X-band and Ka-band," *IEEE Access*, Vol. 8, 30 643–30 654, 2020.

[21] Helena, D., A. Ramos, T. Varum, and J. N. Matos, "The use of 3D printing technology for manufacturing metal antennas in the 5G/IoT context," *Sensors*, Vol. 21, No. 10, 3321, 2021.

[22] Aragbaiye, Y. M., A. Mansoori, C. Shafai, and D. Isleifson, "Implementing a prototype of a short-backfire antenna using additive manufacturing," in *2022 IEEE International Conference on Wireless for Space and Extreme Environments (WiSEE)*, 35–38, Winnipeg, MB, Canada, 2022.

[23] Zhang, Q., S. Xu, J. Heo, E. Altanzaya, G.-Y. Ariunbold, D. Otgonbat, C.-S. Lee, B.-C. Ahn, S. Li, and S.-G. Choi, "Computational design of a broadband in-line coaxial-to-rectangular waveguide transition," *Applied Sciences*, Vol. 14, No. 1, 74, 2023.

[24] Zhang, C. W. and Z. L. Ma, "A 3-D printed wideband waveguide based circularly polarized antenna," in *2021 International Conference on Microwave and Millimeter Wave Technology (ICMMT)*, 1–2, Nanjing, China, 2021.

[25] Aziz, M., A. El Hassan, M. Hussein, E. Zaneldin, A. H. Al-Marzouqi, and W. Ahmed, "Characteristics of antenna fabricated using additive manufacturing technology and the potential applications," *Heliyon*, Vol. 10, No. 6, e27785, 2024.

[26] Sharma, A., "3D printed X-band antenna for the interstellar mapping and acceleration probe (IMAP) spacecraft," in *2023 International Conference on Electromagnetics in Advanced Applications (ICEAA)*, 487–487, Venice, Italy, 2023.

[27] Gupta, S. K. and A. Bage, "A compact, dual-band antenna with defected ground structure for 5G applications," *Journal of Circuits, Systems and Computers*, Vol. 30, No. 16, 2150298, 2021.

[28] Jocqué, J., Q. Van den Brande, S. Luchie, B. Van Herbruggen, E. De Poorter, J. Verhaevert, S. Lemey, P. Van Torre, and H. Rogier, "Resource-efficient simulation framework for accurate UWB antenna system design," *IEEE Internet of Things Journal*, Vol. 12, No. 9, 11 441–11 456, 2024.

[29] Kotzé, K. and J. Gilmore, "SLM 3D-printed horn antenna for satellite communications at X-band," in *2019 IEEE-APS Topical Conference on Antennas and Propagation in Wireless Communications (APWC)*, 148–153, Granada, Spain, 2019.

[30] Olivová, J., M. Popela, M. Richterová, and E. Štefl, "Use of 3D printing for horn antenna manufacturing," *Electronics*, Vol. 11, No. 10, 1539, 2022.

[31] Yohandri, , R. A. Syafrindo, J. T. S. Sumantyo, C. E. Santosa, and A. Munir, "3D print X-band horn antenna for ground-based SAR application," in *2017 Progress In Electromagnetics Research Symposium — Spring (PIERS)*, 1250–1253, St. Petersburg, Russia, 2017.